ISSN 1063-7729, Astronomy Reports, 2016, Vol. 60, No. 10, pp. 939–948. © Pleiades Publishing, Ltd., 2016.
Original Russian Text © M.A. Livshits, I.Yu. Grigoryeva, I.I. Myshyakov, G.V. Rudenko, 2016, published in Astronomicheskii Zhurnal, 2016, Vol. 93, No. 10, pp. 907–917.

Evidence for a Relationship between Emerging Magnetic Fields, Electric Currents, and Solar Flares Observed on May 10, 2012

M. A. Livshits[1*], I. Yu. Grigoryeva[2], I. I. Myshyakov[3***], and G. V. Rudenko[3]**

[1] *Pushkov Institute of Terrestrial Magnetism, the Ionosphere and Radio Wave Propagation, Russian Academy of Sciences, Troitsk, Moscow, Russia*

[2] *Central (Pulkovo) Astronomical Observatory, Russian Academy of Sciences, Pulkovo, St. Petersburg, Russia*

[3] *Institute of Solar–Terrestrial Physics, Siberian Branch, Russian Academy of Sciences, Irkutsk, Russia*

Received December 18, 2015; in final form, February 17, 2016

Abstract—Multi-wavelength observations and magnetic-field data for the solar flare of May 10, 2012 (04 : 18 UT) are analyzed. A sign change in the line-of-sight magnetic field in the umbra of a small spot has been detected. This is at least partly associated with the emergence of a new magnetic field. A hard X-ray flare was recorded at almost the same time, and a "sunquake" was generated by the impact of the disturbance in the range of energy release on the photosphere. A sigmoid flare was recorded at the beginning of the event, but did not spread, as it usually does, along the polarity inversion (neutral) line. SDO/HMI full vector magnetic-field measurements are used to extrapolate the magnetic field of AR 11476 into the corona, and to derive the distribution of vertical currents j_z in the photosphere. The relationship between the distribution of currents in the active region and the occurrence of flares is quite complex. The expected "ideal" behavior of the current system before and after the flare (e.g., described by Sharykin and Kosovichev) is observed only in the sigmoid region. The results obtained are compared with observations of two other flares recorded in this active region on the same day, one similar to the discussed flare and the other different. The results confirm that the formation and eruption of large-scale magnetic flux ropes in sigmoid flares is associated with shear motions in the photosphere, the emergence of twisted magnetic tubes, and the subsequent development of the torus instability.

DOI: 10.1134/S1063772916090031

1. INTRODUCTION

Over the past 15 years, the TRACE, RHESSI, CORONAS-F, and other spacecraft have provided a wealth of data on nonstationary processes in the Sun. The characteristics of X-ray sources and their relationship with the microwave and optical emission of solar flares have been studied in detail [1]. It was believed over the past 50 years that these events occurred in the corona, and were due to the reconnection of magnetic-field lines. However, recent observations of the full vector magnetic field with Hinode, SDO/HMI, and AIA [2, 3] and theoretical extrapolations of photospheric magnetic fields to the corona [4] have shown that, during the evolution of active regions (ARs), magnetic-field energy is accumulated at very low altitudes in the chromosphere, where Lorentz forces operate and electric currents are significantly amplified. The free energy of the currents is released at low altitudes, giving rise to flares, coronal mass ejections (CMEs), and "sunquakes." This leads us to turn away from the idea of "coronal flares" and return to the notion of chromospheric flares, which was widespread in the 1960s and 1970s. This idea is supported even by the advocates of reconnection as a mechanism for the observed flares [5].

Following the earliest measurements of solar magnetic fields, Severnyi [6] showed that the sources of individual flare nodes in the chromosphere are located in the vicinity of polarity-inversion lines. He and his co-authors showed that these nodes arise in areas of high-magnetic magnetic-field gradients. The first measurements of the full vector magnetic fields of solar ARs enabled studies of the relationship between electric currents and the evolution of solar flares. However, the correlation between the distribution of the vertical magnetic field and chromospheric Hα flare nodes proved to be very complex. It is only now that the problems discussed by Severnyi [6] and

*E-mail: maliv@mail.ru
**E-mail: irina.2014.irina@mail.ru
***E-mail: rud@mail.iszf.irk.ru

Rust [7] can be investigated in some detail using modern observations of magnetic-field dynamics, multi-wavelength observations of flares, and new theoretical concepts about electromagnetic processes in the Sun.

Recent studies of the relation between the evolution of magnetic fields and nonstationary processes have been based on a number of earlier results. The detection of the emergence of new magnetic fields was important. Change in the field configuration can result in sudden releases of energy, or can intensify the emission of impulsive flares, accompanied by the generation of plasma motions (CMEs, etc.) and EUV waves (sunquakes). Plasma in the chromosphere may be heated by current dissipation [8], Lorenz forces [9], or the energy lost by accelerated particles at the onset of the gas-dynamical response, as was first considered by Kostyuk and Pikelner [10]. An important fact for our understanding of the nature of these nonstationary processes is that a large-scale flux rope sometimes emerges before or during a flare, usually in the vicinity of the polarity-inversion line, leading to the occurrence of a sigmoid flare (see ([11], and references therein) and the subsequent formation of post-eruption arcades.

Thus, theoretical developments and the appearance of new observational data require new concepts about the development of MHD processes in the outer atmosphere of the Sun. These must take into account the direct effects of currents on heating and plasma motions in the chromosphere and the characteristic behavior of plasma in force-free and potential fields in the corona, including the possibility of magnetic reconnection and the formation of thin current sheets. The structures of current systems in ARs are of primary importance here, taking into into account the topology of the magnetic fields in ARs or activity complexes, as was studied in [12]. Sudden reconstructions of the magnetic configuration are closely related to the development of nonstationary phenomena. The role of shear motions in such reconstructions was considered earlier in [13] (see also the subsequent discussions in [14]), usually for processes involving reconnection in the corona. Observations of the ejectionof twisted flux ropes and the simulations of [11] indicate the character of such reconstructions of magnetic configurations and current systems.

Of course, it is important to find observational evidence that supports or disproves these new theoretical ideas. One of the first studies in this context was [15, Fig. 10], which represents schematically a current system with vertical currents j_z of opposite signs on either side of the polarity-inversion line. This picture would be expected in the simplest case of a transition from a twisted flux rope to the post-eruption phase of a flare. However, numerous full vector magnetic-field measurements that have been used to reconstruct the distribution of the vertical currents j_z are now available for many active regions. As in the pioneering work of Severnyi, throughout the ARs, these current distributions do not correspond to this ideal pattern.

In our current study, we have investigated the relationship between currents and the development of non-stationary processes, using the events observed on May 10, 2012 as an example. The first flare, with its maximum at 04 : 18 UT (GOES), was unusual, since the emergence of new field was observed in the umbra of a small spot, simultaneous with a hard X-ray flare. This event was accompanied by a sunquake. The second observed flare, with its maximum at 05 : 10 UT, was more typical, while the third observed flare (20 : 26 UT) was similar to the first, but less powerful. The emission of the first flare is analyzed in Section 2. Observations of the emergence of magnetic field at 04 : 00 UT are analyzed in Section 3. The behavior of the photospheric and coronal magnetic fields is discussed in Section 4, and the data are briefly compared with those for the two subsequent flares in Section 5. In Section 6, we discuss the origin of and a possible model for sigmoid flares involving the ejection of large, twisted magnetic ropes.

2. EMISSION OF THE FLARE OF MAY 10, 2012 (04 : 18 UT)

AR 11476 appeared on the solar disk on May 5, 2012, and its area had reached 1000 msh by May 10. The corresponding sunspot group consisted of a large, complex leading spot and small spots at the center and in the trailing part of the group. On May 10, the AR produced two large M flares and a series of weak flares of class C. We consider here the first flare, which had magnitude M5.7 (04 : 11–4 : 23, maximum at 4 : 18 UT, GOES), and compare it with C7.9 flares that occurred during the decay of the first flare and with an M1.7 flare observed in the same AR on the evening of that same day (Fig. 1).

The first flare displayed ordinary X-ray and microwave characteristics. It occurred in the immediate vicinity of a small spot at the center of the group, near the polarity-inversion line, had an impulsive nature, and was fairly hard.

The left panel of Fig. 2 presents the entire AR 11476 in white light (SDO/HMI Ic). The rectangle on the right delineates region A, where the flare was observed, and the square on the right region B, where a change in the sign of the magnetic signal was recorded in the line-of-sight magnetogram (SDO/HMI LOS). The same flare is shown on the

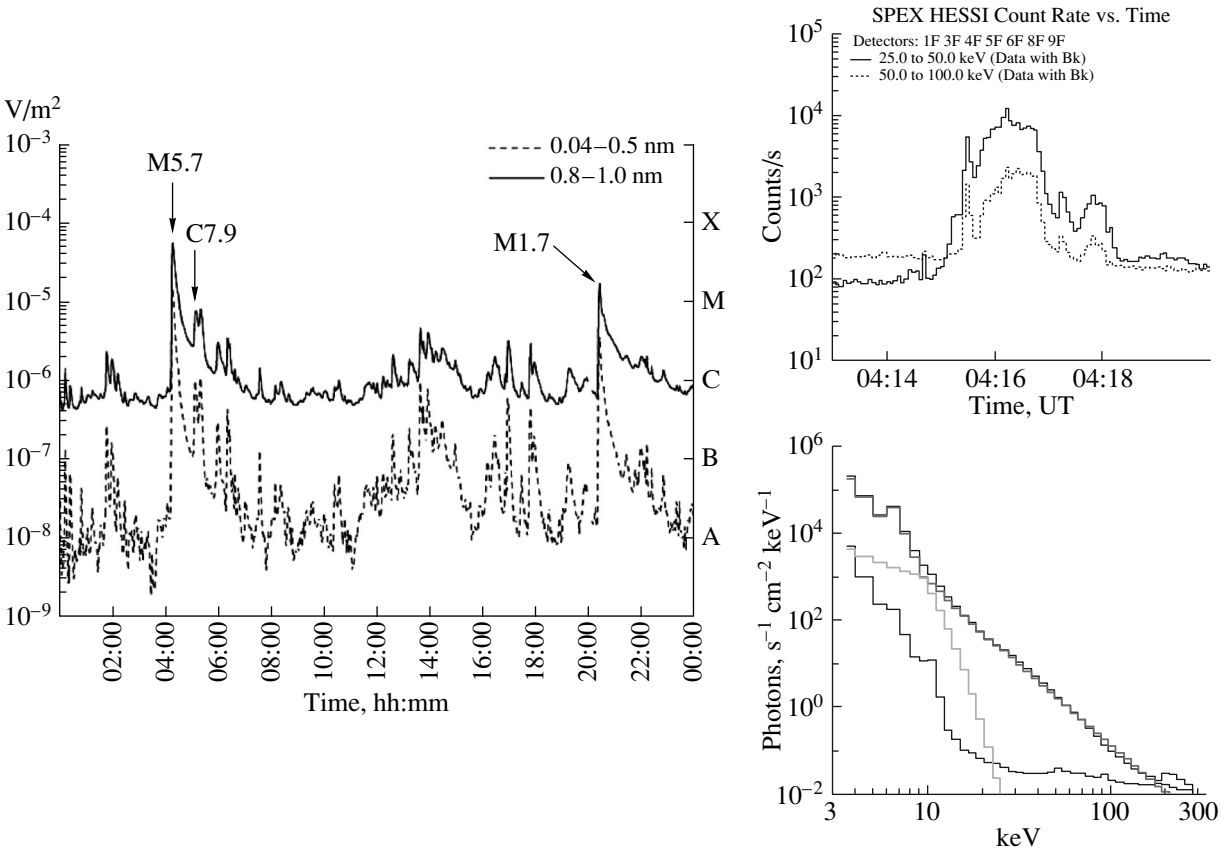

Fig. 1. Left: time profiles of the one-minute GOES data for May 10, 2012; the arrows mark the studied flares. Top right: RHESSI HXR time profiles at 25–50 keV (solid) and 50–100 keV (dotted). Bottom right: the flare spectrum at 04 : 15 : 44 UT on May 10, 2012. The thermal emission and background are also shown.

right in the 131 Å line (SDO/AIA) during the growth phase of its intensity.

In general, judging by the GOES and RHESSI X-ray emission [16], this was a typical event that was somewhat harder than an average M5 flare (Fig. 1; the slope of the photon spectrum is $\gamma \approx 303.0$ at 20–80 keV).

Temporal profiles of the intensity (Stokes I) and polarization (Stokes V) at 17.0, 9.4, 3.75, and 2.0 GHz based on data from the Nobeyama polarimeter (NoRP: [17, 18]) are presented in the left and center panels of Fig. 3. The fluxes and their dynamics correspond to those of most flares of this strength. As usual, there are two discernible footpoints of the flare loop, located in magnetic fields with opposite signs (Fig. 3, right). At the same time, the behavior of the polarization is somewhat more complex. For example, a change in the sign of the polarization is detected at 9.4 GHz, and a sudden sign change is observed at 2 GHz at 04 : 16 UT. This evolution of the polarized microwave emission is presumably associated with a complex topology of the AR in the lower corona (see below).

3. EMERGENCE OF MAGNETIC FIELD

In many cases, a relationship is observed between the occurrence of flares and the emergence of new magnetic field. However, these two processes do not usually coincide in time and space. In other words, the emergence of new magnetic field disrupts the stability of the magnetic configuration. A flare in a given AR may occur fairly far from the emerging field, before or after its emergence, or even between separate flare episodes. In the case considered here, the two processes coincided in space and time. Moreover, although new magnetic field usually appears in the vicinity of the polarity-inversion line separating "hills" corresponding to fields with modest intensities, in our case, the emergence of new field occurred in the umbra of a small spot near the AR's center, delineared by the square (region B) in Fig. 2. Here, the sign change of the signal (SDO/HMI LOS) indicates the emergence of new field, but does not necessarily imply a reversal of the sign of the field.

Our analysis of the Stokes parameters recorded in the presumed region of field emergence indicates that they follow Gaussian distributions. Of course, strong

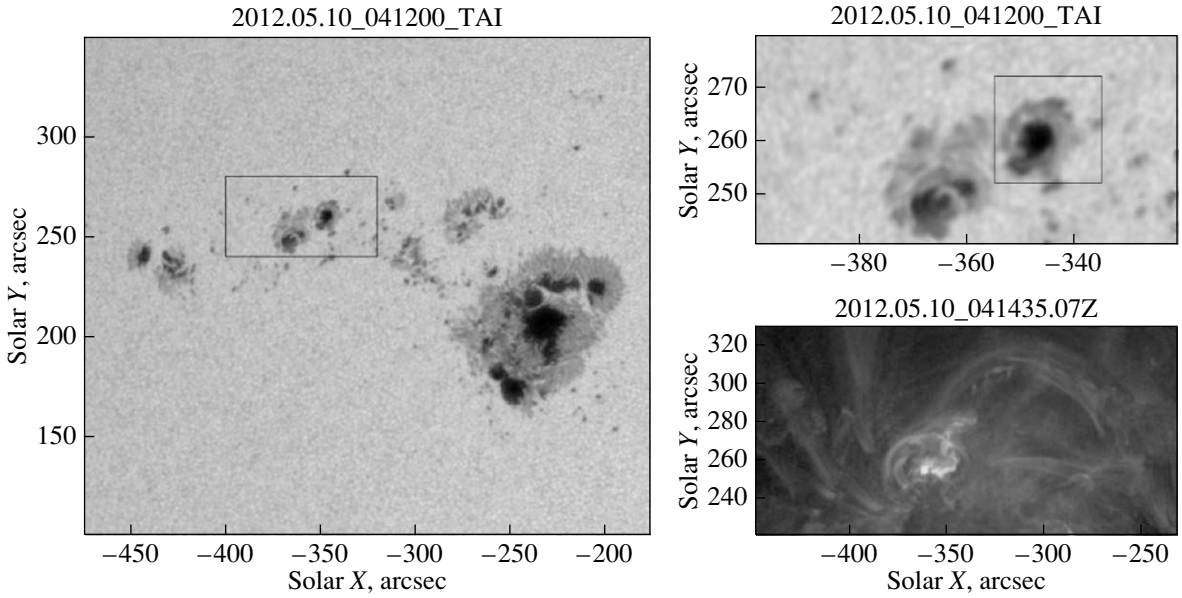

Fig. 2. Left: the sunspot group in AR 11476 at 04 : 12 UT (SDO/HMI Ic). The rectangle shows region A. Right: region A with region B shown by the square, for the same time (top); flare in the 131 Å line (SDO/AIA) near the maximum (bottom). The scales show the distance from the disk center in arcsec.

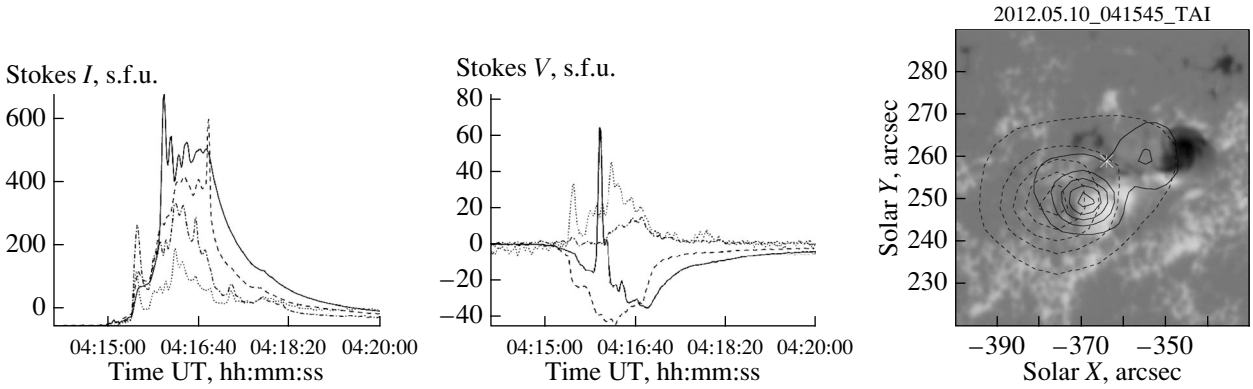

Fig. 3. Left and center: Evolution of the microwave flux from the M5.7 flare on May 10, 2012 (Stokes parameters I and V) at 2 GHz (solid), 3.75 GHz (dashed), 9.4 GHz (dot-dashed), and 17 GHz (dotted) (Nobeyama, NoRP). Right: fragment of the LOS magnetogram of the flare-generation region at the time of maximum. The scales indicate the distance from the disk center in arcsec. The contours correspond to the emission at 34.0 GHz (solid) and 17.0 GHz (dashed) (Nobeyama, NoRH) at 04 : 15 : 30 UT; the contours correspond to 90%, 70%, 50%, 30% and 10% of the maxima at 17 GHz and 34 GHz. The asterisk shows the flare site according to the RHESSI HXR data.

plasma flows may interfere with the field measurements. One of the arguments for the reality of this field emergence is that a similar pattern was observed during a flare recorded at this same location in the same AR at 20 : 26 UT on the same day.

Figure 4 shows the evolution of the emerging field in region B at selected times, based on the SDO/HMI LOS magnetogram data. The reversed sign of the signal was observed during 4 minutes, after which the sign returned to its original value for another 4 minutes. Unfortunately, full vector magnetic-field data are available only for times before and after the maximum effect in the signal for the LOS magnetograms. Note that the upward movement registered according to the SDO frame 04:16:30 UT.

A sunquake was registered in the vicinity of the hard X-ray maximum during this event [19]. This response to the sudden energy release in the photosphere was projected onto a point at the peak of a low flare loop. The asterisk in the right panel of Fig. 3 marks the position of the hard X-ray source at the maximum of the flare. The contours of the 17.0 and 34.0 GHz radio brightness superimposed on the distribution of the line-of-sight magnetic field

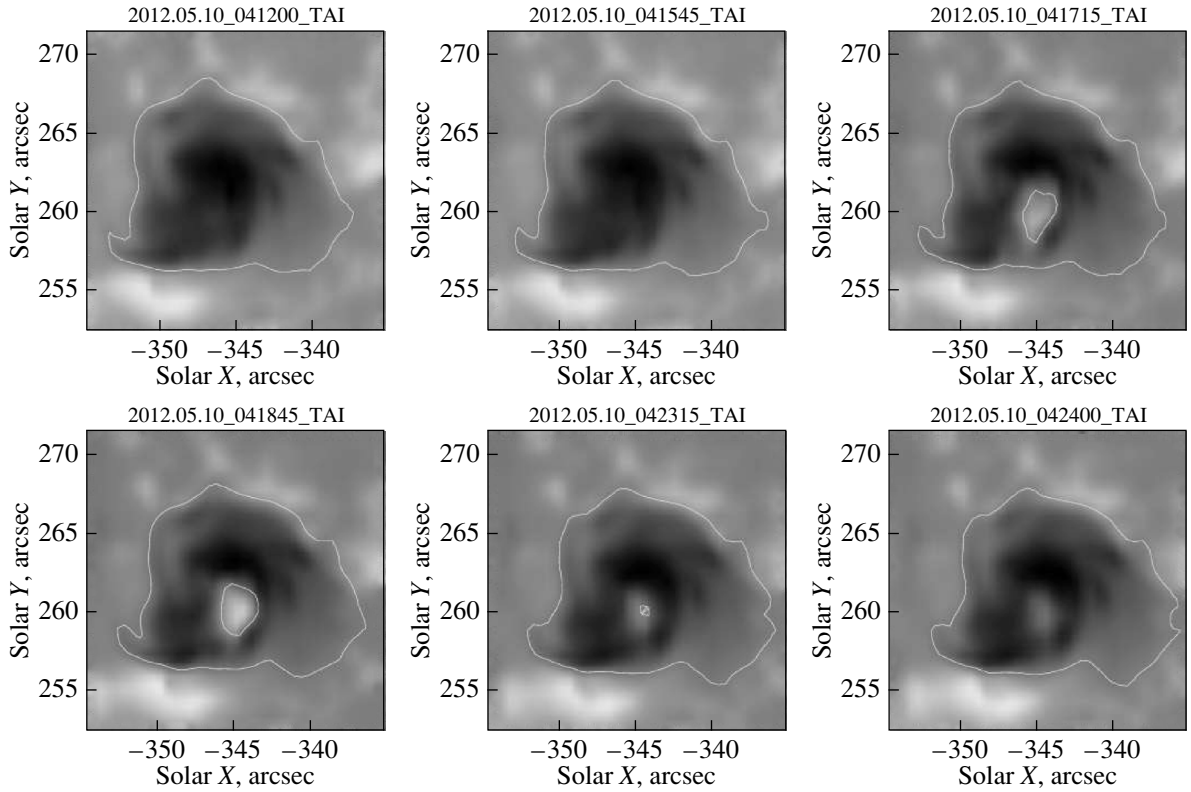

Fig. 4. Fragments of the image of the line-of-sight magnetic field in the region of emerging field in AR 11476 on May 10, 2012 (SDO/HMI LOS) at selected times during the flare, from 04 : 12 : 00 UT through 04 : 24 : 00 UT. The contours show the local magnetic field along the polarity-inversion line. The scales indicate the distance from the center of the disk in arcsec.

at the event maximum were constructed using data from the Nobeyama radio heliograph (NoRH, [20]). The footpoints of the low flare loop seen in various SDO/AIA ranges are most pronounced at 34.0 GHz. In this case, the sunquake is most likely tied to the time and site of the primary energy release. This is consistent with the sunquake data of [15, 21].

4. EXTRAPOLATION OF THE FIELDS TO THE CORONA AND THE DISTRIBUTION OF CURRENTS IN AR 11476

Our understanding of the role of magnetic fields in the development of activity in the outer atmosphere of the Sun has changed in recent years. The magnetic β parameter (the ratio of the gas to the magnetic pressure), which is close to unity just above the photosphere, becomes very small in the chromosphere and corona. As a result, the plasma at the base of an active region is subject to Lorenz forces, while the field higher up becomes force-free. During the evolution of fields at chromospheric heights, a significant excess of the magnetic-field energy over the corresponding force-free (potential) value can arise, and this free energy can contribute to the development of nonstationary processes.

Full vector magnetic-field observations in the photosphere can be used to extrapolate the nonlinear force-free fields to coronal heights. This nonlinear force-free field (NLFFF) extrapolation method is widely used in solar physics (e.g., see [4]).

In our work, we calculated the coronal magnetic field in the NLFFF approximation using an optimisation method that was first proposed in [22] in the form realized in [23]. The essence of this method is the successive transformation of an initial (potential) distribution of the magnetic field toward a force-free structure, in accordance with the photospheric magnetogram. A functional of the following form is introduced:

$$L = \int\limits_V \left[B^{-2}|[\nabla \times \mathbf{B}] \times \mathbf{B}|^2 + |\nabla \cdot \mathbf{B}|^2\right] dV, \quad (1)$$

which vanishes if the field B is force-free and is positive otherwise. Thus, in the course of finding the minimum of the functional (1), the field in the volume V acquires a force-free configuration. We used a potential field calculated from the normal component of the photospheric field via a fast Fourier transform (FFT) as the initial distribution. A distinguishing feature of this realization of the optimisation method

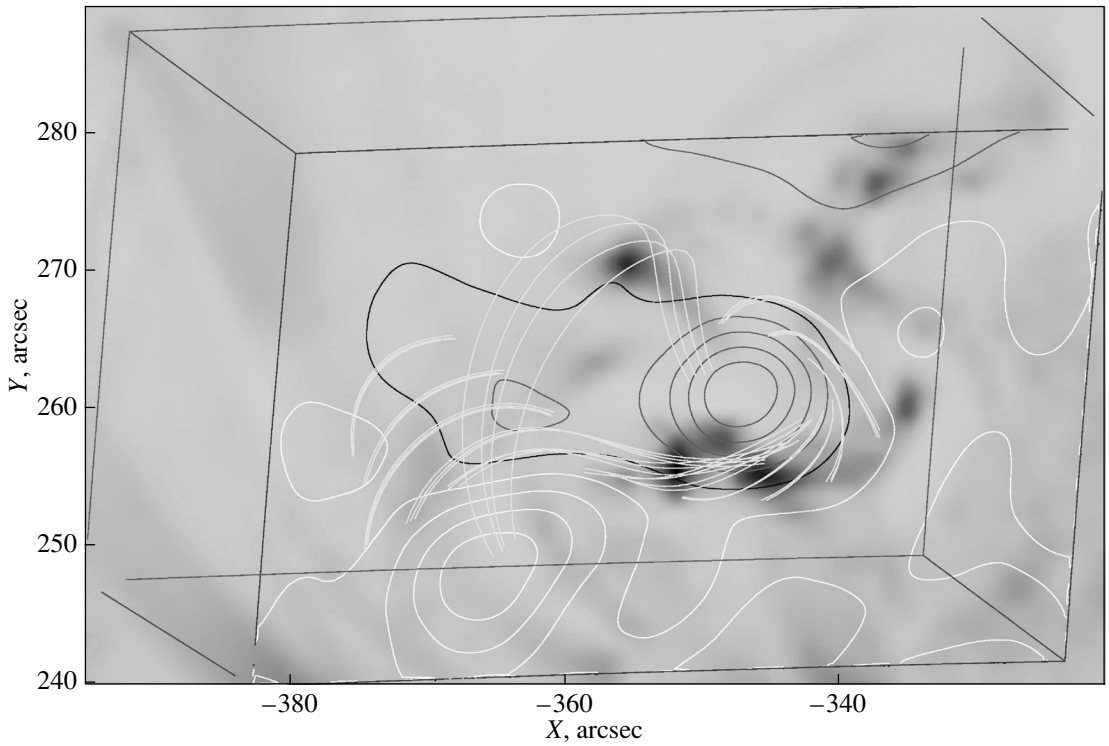

Fig. 5. The background shows a fragment of the negative image of AR 11476 in the 171 Å EUV line obtained on May 10, 2012 at 04 : 12 : 00 UT (SDO/AIA). The contour lines show the positive (white) and negative (black) line-of-sight magnetic field in the flare region at the same time, at 80%, 60%, 40%, and 20% of the maximum. The field lines above the neutral line and higher loops connecting the hills of magnetic field of opposite signs are also shown in white. The straight lines show the projection of a cube. The scales indicate the distance from the center of the disk in arcsec.

is the use of a full system of evolutionary equations for the field (see [23]). Thus, the field distribution at the upper and lateral boundaries of the computational domain, which is not initially determined by the measurements, varies during the computations. This approach makes it possible to enhance the quality of the field reconstruction.

Figure 5 shows the result of calculating the field lines in region A (Fig. 2) to a height of 25 000 km. At the very beginning of the flare, the field lines around the hill of field in the small spot are concentrated along the polarity-inversion line. The flare nodes formed in the region of highest field concentration (see the 171 Å image in Fig. 5). Generally speaking, a braid of field lines encompassing a significant fraction of the neutral line forms in many flares, especially where it separates hills of strong magnetic field. In our case, we suppose that a small braid formed only on the southern side of the small spot at the center of the group. As in other sigmoid flares, this shape for the field lines in AR stimulates the development of a sigmoid flare. In this case, the field reconstruction occurred almost immediately after the formation of currents above the neutral line.

Figure 5 shows only closed field lines in the region A projected onto the plane of the sky. We can see a small spot of negative polarity surrounded by a concentration of field lines that continue beyond the neutral line. It is currently believed that this is where the main force-free currents that are usually identified with the plasma flux rope flow. It is important that this concentration of field lines coincides with the positions of flare nodes forming a small sigmoid.

The NLFFF extrapolation (Fig. 5) shows that, in addition to low field lines, there are also field lines rising to 5000 km or more, which connect the small spot of negative polarity with the hill of positive polarity. These are located above the rope of field lines, possibly preventing the development of an ejection. In the course of the flare evolution inferred from the SDO/AIA EUV data, flare loops with heights of 10 000–20 000 km formed, but the plasma did not escape into interplanetary space (i.e., there was no CME).

We than calculated the distribution of vertical currents j_z at the photosphere level throughout the AR on May 10, 2012 for the time interval from 03 : 48 UT to 05 : 48 UT using full vector magnetic-field data in steps of 720 s. Analysis of the location of the flares on that day confirms the correlation between the

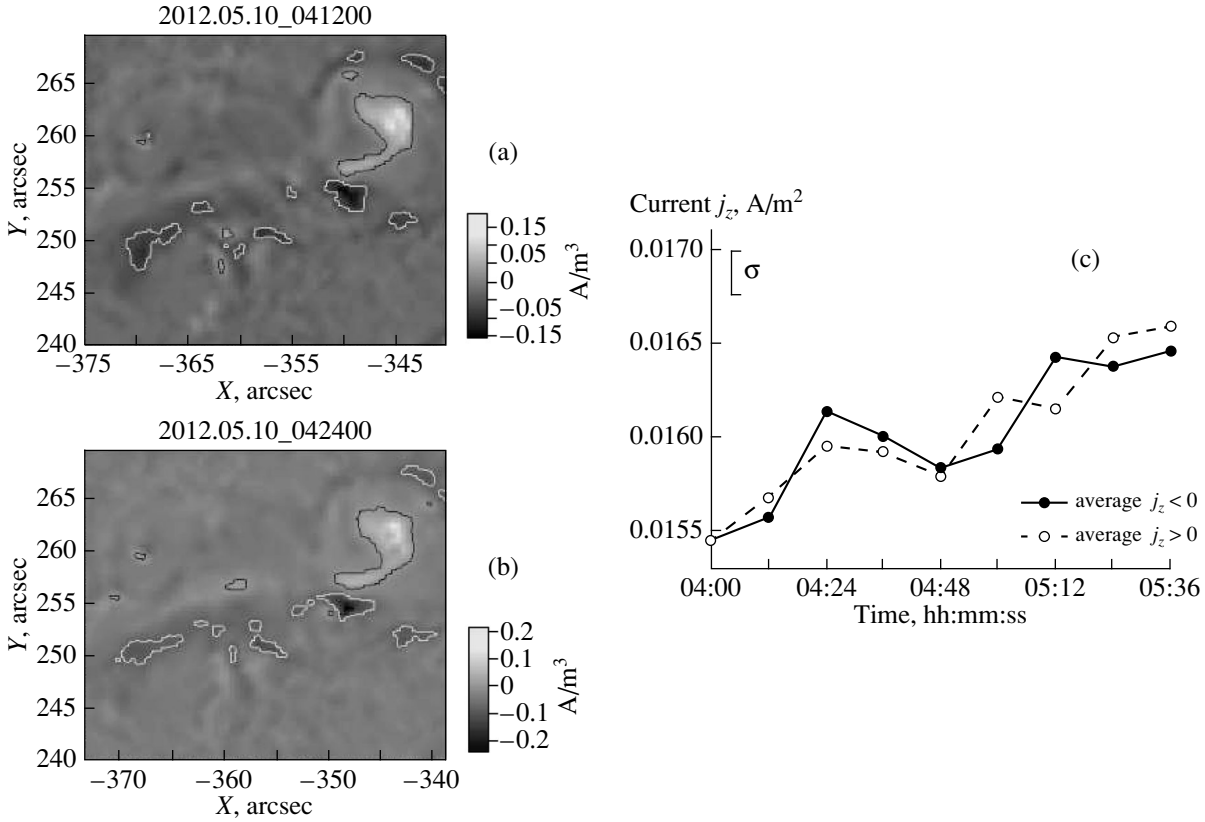

Fig. 6. Left: the background shows fragments of maps of the vertical currents j_z calculated for 04 : 12 UT and 04 : 24 UT, before and after the flare maximum, and the contours show levels of $j_z \pm 0.05$ A/m^2. The scales indicate the distance from the disk center in arcsec. Right: evolution of the mean currents $j_z > 0$ (solid) and $j_z < 0$ (dashed) on May 10, 2012. The modulus $|j_z|$ is shown for negative magnetic fields. The vertical bar shows the measurement uncertainties.

flare sites and the regions of enhanced current [24]. However, no definite regularity was observed in the behavior of the currents in the AR as a whole and the occurrence of flares: all the currents were concentrated along the neutral line, including the region near the spots. Therefore, changes that may occur in the middle of the neutral line in the AR become lost among the total currents of both signs. Sharykin and Kosovichev [15] noted that, in an "ideal" current system, the mean currents of each sign should increase on either side of a polarity-inversion line. In our case, as in studies of the relationship btween vertical currents and flares in the 1970s, this effect is very weak with respect to the entire AR.

Since the strongest field variations in the growth phase of the flare were observed at the site of the sigmoid, we studied this effect inside region A (see Fig. 1). Figure 6 illustrates the distribution of vertical currents in the photosphere at two times. The currents of different sign come into contact at 04 : 00 UT at the point $Y = 256''$, $X = 350''$. This coincides with the region of field-line concentration in Fig. 5, above the polarity-inversion line in the region of strong fields.

Generally speaking, the variations of the pattern of currents can be traced on the set of j_z maps constructed using the data on the full vector magnetic field. The largest variation of the currents takes place in the region of the sigmoid. The subsequent evolution of the current system is tightly related to the development of numerous weak flares in AR 11476. Note also that substantial changes in the currents occurred at 04 : 00–04 : 24 UT near $Y = 250''$, $X = 364''$, which is the footpoint of the loop connecting the place where the magnetic field emerges and the hill of positive polarity (see Fig. 5).

Apart from the changes in the current pattern, certain differences between the two images in the left panel of Fig. 6 are manifest in all the current values, which in this example, is reflelcted even in the difference of scales. To study this effect, we determined the mean value of the vertical current in the entire region A. The averaging was carried out separately for pixels with positive and negative field. The general trend of the averaged vertical current j_z of both signs in the time interval from 04 : 00 UT to 05 : 48 UT can be seen in Fig. 6c. The overall trend reflects the gradual

increase in the flaring activity of this AR on the given day.

This effect related to the flare in question is manifest as an increase in the mean current during the flare, 04 : 00–04 : 24 UT. According to the hard X-ray data, the maximum of the flare occurs at 04 : 16 : 30 UT (see Fig. 1). In our case, the maximum signal corresponds to 04 : 24 UT, after which the signal falls. This character of the j_z variations is noted in [15] as well. The maximum value is small, and only slightly exceeds 3σ ($\sigma \simeq 2.3 \times 10^{-4}$ A/m^2, and is determined by the change in the current in an area of the same AR in the quiescent state).

Note also that the indicated flare maximum occurred between 04 : 12 UT and 04 : 24 UT. Unfortunately, no freely available data on the full vector magnetic field with better time resolution are available, so that our estimate of the change in the current characteristics during this flare may be somewhat underestimated.

5. THE OTHER FLARES OF MAY 10, 2012

AR 11476 displayed a high level of flare activity during the time in question. It produced a large number of weak C flares on every day beginning with May 6, producing one or two M flares on some days up until May 17.

Apart from the M5.7 flare analyzed here, on the same day, AR 11476 produced 16 C flares and one M1.7 flare, registered at 20 : 20 UT. A change in the SDO/HMI LOS line-of-sight magnetic-field signal was registered in the umbra of the same small spot as the one in which the first M flare occurred. The duration of this effect was about a factor of two shorter than for the first flare (from 20 : 24 UT to 20 : 29 UT). However, unlike the M5.7 flare, the HMI LOS magnetogram signal in the region of field emergence did not change sign.

This M1.7 flare was also fairly hard. The FERMI space mission recorded emission near energies of 100 keV. At the same time (about 20 : 24 UT), significant emission at energies above 50 keV, with a maximum of more than 2000 pulses/second, was recorded by the Suzaku spacecraft (see the catalog http://www.astro.isas.jaxa.jp/suzaku/HXD-WAM/WAM-GRB/solar/untrig/120510202227.html). Thus, the conditions leading to "fast" sigmoid events can arise in an AR over a period of from several hours to a day.

Most of the class-C flares C on May 10, 2012 had a different origin than the M flares. Let us consider by way of example a C7.9 flare that was observed during the decay of the soft X-ray emission associated with the main event considered. This flare occurred at 05 : 04 UT above the neutral line, between the spots we are analyzing and the leading spots. The flare nodes then extended from this point directly to a large spot. These weak events may have been triggered by activity in this large spot. In some cases, this activity is due to the emergence of new field in the vicinity of the spot, the rotation of the spot, or simply the formation of new magnetic hills. Some of these weak events are fairly hard, but they usually occur during the decay of the soft X-ray emission from major flares. Their hardness is due to the presence of conditions more favorable for particle acceleration in traps, where some electrons with energies above 10 keV are still present after the previous event [25].

6. RESULTS AND DISCUSSION

Our conclusions are as follows.

(1) In the event analyzed here, there was essentially a pulse-like release of energy accompanied by bursts of hard X-ray and microwave emission. Simultaneously, the response of the photosphere was registered in the form of a sunquake. There is reason to believe that the formation of a sigmoid flare began at the same time, but was not completed. Similar processes were repeated in the second M flare at 20 : 20 UT, but were absent from many weak C flares in other parts of this AR.

(2) Full vector magnetic-field data were used to calculate the vertical currents throughout the AR. The trend displayed by the currents reflects the overall development of the flaring activity of the AR on that day. The simple pattern of the current system [15] arising during the flare, after the transformation of the currents above the neutral line into loop currents located high above the photosphere, arranged at a large angle to the neutral line, and closing beneath the photosphere, does not agree with the calculated values for the currents. However, if such calculations are carried out in an area confined to the size of the flare sigmoid, we find local maxima in the time variations of both the positive and negative vertical currents. This may testify to variations in the system of currents.

(3) The examples of the two moderate-power M flares considered here demonstrate that both sunquakes and particle acceleration operate more efficiently in the fairly strong magnetic fields residing near the polarity-inversion line.

We will now briefly discuss the connection between our results and the general problem of the development of non-stationary processes. The physics of sigmoid flares has been widely discussed in the literature. Rich experience from numerical simulations of these processes has been accumulated (e.g., see [11] and references therein). Many earlier studies

employed the idea of magnetic reconnection. It is now believed that the main factor is current dynamics, with the role of reconnection becoming important at high altitudes in the corona. The earlier conclusion that plasma flux ropes with currents are not ejected directly from the top of the convection zone remains valid. Large-scale sub-photospheric motions shear the feet of field lines along polarity-inversion lines. In addition, helicity is also carried outward from sub-photospheric layers.

Thus, the outward transport of shear and helicity from beneath the photosphere creates the conditions for the formation of a magnetic flux rope. Both theoretical reasoning and NLFFF extrapolations of fields to the corona suggest that the evolution of AR magnetic fields described above leads to the accumulation of some amount of free energy in the chromosphere, which can be spent on the development of nonstationary processes.

The moment of a large impulsive flare is associated with the reconstruction of the current system in the AR. Namely, a bunch of field lines and the currents flowing along them change appreciably, approaching an ideal configuration; i.e., currents flowing along loops lying at large angles to the neutral line in projection on the photosphere.

The magnetic configuration essentially returns to its original state after the flux rope is ejected. If the previously existing large-scale sub-photospheric motions continue, the formation of a flux rope is repeated; i.e., a series of similar flares develops. These pictures are in agreement with the results of the latest numerical calculations [26].

Of course, one important question is the flare mechanism itself. Note that, preceding a flare, the strong current in the magnetic rope should close in sub-photospheric layers. This suggests a toroid in the meridianal plane, which has partially risen above the photosphere. This geometry for the twisted magnetic field is depicted in Fig. 2 of [27].

In general, flux ropes can exist over long times, even in active regions with fairly complex topologies. However, in some cases, especially in the presence of strong currents, the torus instability can arise [28]. The conditions required for the development of such instabilitie have been determined in laboratory experiments [29]. Naturally, we cannot insist upon the existence of a specific type of instability under the conditions in flares on the Sun and low-mass stars. It is more resonable to consider the more general case of hydrodynamical instabilities in a plasma rope with a strong current.

Simulations of current systems throughout an entire AR is currently an important task. It has only now become clear that strong currents and Lorenz forces exist at very low heights (up to 2000–3000 km above the photosphere). Higher in the corona, the fields rapidly become potential, with the possible presence of thin current sheets.

In addition to the above general considerations, additional evidence for this is provided by the complex behavior of the polarization of the associated microwave radiation, which changes sign in the transition from the disk center to the limb. This is due to the beam entering into a region of quasi-transverse magnetic field (a QT region; e.g., see [30]). In our case (see Fig. 3) we see a change of the polarization sign at 9.4 GHz at the same time (without motion of the source).

In addition to this well-known effect, a secondary short-time sign change was registered at 2 GHz, with the maximum of the polarized emission occurring at 04 : 16 UT. This, in turn, suggests a complex coronal magnetic-field topology, with the complex polarization picture being due to both projection effects (as occurs in the passage of a QT region, e.g., [31]) and to increasing complexity of the coronal topology of the AR.

Thus, an "ideal" current system can exist within a small volume, but it is usually immersed in a collection of independent magnetic fluxes that are divided by separatrix surfaces. As a result, the characteristics of the polarized emission at low microwave frequencies indicate a role for reconnection in the coronal layers in the AR. Note that the foundations for studies of the topology of the solar corona were laid in [12].

We also note that two scenarios for the development of non-stationary processes are possible in the Sun: (1) more often with the formation of CMEs (especially in powerful flares) and (2) less often with a rising loop, without an outward transport of matter. The latter case was observed in the M flares that occurred on May 10, 2012.

ACKNOWLEDGMENTS

We thank the reviewers and to V.I. Vybornov for his assistance in the course of this work. The SDO data were provided courtesy of NASA and the HMI and AIA science teams. We acknowledge the use of RHESSI and GOES X-ray data. We also thank the instrumental teams operating the Nobeyama solar facilities.

This work was supported by the Russian Foundation for Basic Research (projects 14-02-00922, 16-32-00315mol-a, 15-32-20504mol-a-ved, 15-02-03835a, 15-02-01089a, 15-02-01077a, and 16-02-00749a) and by the Presidium of the Russian Academy of Sciences.

REFERENCES

1. S. Krucker, M. Battaglia, P. J. Cargill, L. Fletcher, H. S. Hudson, A. L. MacKinnon, S. Masuda, L. Sui, M. Tomczak, A. L. Veronig, L. Vlahos, and S. M. White, Astron. Astrophys. Rev. **16**, 155 (2008).
2. J. Schou, P. H. Scherrer, R. I. Bush, J. Schou, P. H. Scherrer, R. I. Bush, R. Wachter, S. Couvidat, M. C. Rabello-Soares, R. S. Bogart, J. T. Hoeksema, Y. Liu, T. L. Duvall, D. J. Akin, B. A. Allard, et al., Solar Phys. **275**, 229 (2012).
3. J. R. Lemen, A. M. Title, D. J. Akin, P. F. Boerner, C. Chou, J. F. Drake, D. W. Duncan, C. G. Edwards, F. M. Friedlaender, G. F. Heyman, N. E. Hurlburt, N. L. Katz, G. D. Kushner, M. Levay, R. W. Lindgren, et al., Solar Phys. **275**, 17 (2012).
4. T. R. Metcalf, M. L. De Rosa, C. J. Schrijver, G. Barnes, A. A. van Ballegooijen, T. Wiegelmann, M. S. Wheatland, V. Gherardo, and J. M. McTtiernan, Solar Phys. **247**, 269 (2008).
5. L. Fletcher, B. R. Dennis, H. S. Hudson, S. Krucker, K. Phillips, A. Veronig, M. Battaglia, L. Bone, A. Caspi, Q. Chen, P. Gallagher, P. T. Grigis, H. Ji, W. Liu, R. O. Milligan, and M. Temmer, Space Sci. Rev. **159**, 19 (2011).
6. A. B. Severnyi, *Some Problems in Solar Physics* (Nauka, Fizmatlit, Moscow, 1988), p. 224 [in Russian].
7. D. M. Rust, Astron. J. **73**, 74 (1968).
8. V. V. Zaitsev and A. V. Stepanov, Phys. Usp. **51**, 1123 (2008).
9. G. H. Fisher, D. J. Bercik, B. T. Welsch, and H. S. Hudson, Solar Phys. **277**, 59 (2012).
10. N. D. Kostyuk and S. B. Pikelner, Sov. Astron. **18**, 590 (1974).
11. A. W. Hood, V. Archontis, and D. MacTaggart, Solar Phys. **278**, 3 (2012).
12. J.-Y. Lee, G. Barnes, K. D. Leka, K. K. Reeves, K. E. Korreck, L. Golub, and E. E. DeLuca, Astrophys. J. **723**, 1493 (2010).
13. Yu. G. Matyukhin and V. M. Tomozov, Sov. Astron. **35**, 79 (1991).
14. E. Priest and T. Forbes, *Magnetic Reconnection. MHD Theory and Applications* (Cambridge Univ. Press, Cambridge, 2000; Fizmatlit, Moscow, 2005).
15. I. N. Sharykin and A. G. Kosovichev, Astrophys. J. **808** (1), id. 72 (2015).
16. R. P. Lin, B. R. Dennis, G. J. Hurford, D. M. Smith, A. Zehnder, P. R. Harvey, D. W. Curtis, D. Pankow, P. Turin, M. Bester, A. Csillaghy, M. Lewis, N. Madden, H. F. van Beek, M. Appleby, et al., Solar Phys. **210**, 3 (2002).
17. K. Shibasaki, M. Ishiguro, and S. Enome, in *Solar Radio Acquisition and Communication System /SORDACS/ of Toyokawa Observatory,* Proc. Res. Inst. Atmosph., Nagoya Univ. **26**, 117 (1979).
18. H. Nakajima, H. Sekiguchi, M. Sawa, K. Kai, and S. Kawashima, Publ. Astron. Soc. Jpn. **37**, 163 (1985).
19. J. C. Buitrago-Casas, J. C. Martinez Oliveros, C. Lindsey, B. Calvo-Mozo, S. Krucker, L. Glesener, and S. Zharkov, Solar Phys. **290**, 3151 (2015).
20. H. Nakajima, M. Nishio, S. Enome, K. Shibasaki, T. Takano, Y. Hanaoka, C. Torii, H. Sekiguchi, T. Bushimata, S. Kawashima, N. Shinohara, Y. Irimajiri, H. Koshiishi, T. Kosugi, Y. Shiomi, M. Sawa, and K. Kai, Proc. IEEE **82**, 705 (1994).
21. I. N. Sharykin, A. G. Kosovichev, and I. V. Zimovets, Astrophys. J. **807**, ID 102 (2015).
22. M. S. Wheatland, P. A. Sturrock, and G. Roumeliotis, Astrophys. J. **540**, 1150 (2000).
23. G. V. Rudenko and I. I. Myshyakov, Solar Phys. **257**, 287 (2009).
24. I. Yu. Grigor'eva, M. A. Livshits, G. V. Rudenko, and I. I. Mysh'yakov, Astron. Rep. **57**, 611 (2013).
25. V. I. Vybornov, I. Yu. Grigor'eva, M. A. Livshits, and E. F. Ivanov, Geomagn. Aeron. **55**, 1112 (2015).
26. A. Savcheva, E. Pariat, S. McKillop, P. McCauley, E. Hanson, Y. Su, and E. E. DeLuca, Astrophys. J. **817**, id. 43 (2016).
27. V. S. Titov and P. Demoulin, Astron. Astrophys. **351**, 707 (1999).
28. V. Shafranov, in *Review of Plasma Physics,* Ed. by M. A. Leontovich (Consultants Bureau, New York, 1966), Vol. 2, p. 103.
29. C. E. Myers, M. Yamada, H. Ji, J. Yoo, W. Fox, J. Jara-Almonte, A. Savcheva, and E. E. Deluca, Nature **528**, 526 (2015).
30. V. V. Zheleznyakov and E. Ya. Zlotnik, Sov. Astron. **7**, 485 (1963).
31. N. G. Peterova and Sh. B. Akhmedov, Sov. Astron. **17**, 768 (1973).

Translated by M. Livshits